Activated Carbon-MnO_2 Composite on Nickel Foam as Supercapacitors Electrode in Organic Electrolyte

Istiqomah [1], *Markus* Diantoro[1,2,*], *Yusril Al Fath*[1], *Nasikhudin* [1], *and Worawat* Meevasana[3]

[1]Department of Physics, Faculty of Mathematics and Natural Science, Universitas Negeri Malang, Jl. Semarang 5, 65145 Malang, Indonesia
[2]Center of Advanced Materials for Renewable, Energy (CAMRY), Universitas Negeri Malang, Jl. Semarang 5, 65145 Malang, Indonesia
[3]School of Physics, Institut e of Science, Suranaree University of Technology, Nakhon Ratchasima 30000, Thailand

Abstract. Since energy storage is an essential component of global energy development, starting with batteries, fuel cells, and supercapacitors, it is an important topic of particular concern. Supercapacitors continue to be developed due to their high power density when compared to batteries, despite all of the benefits and drawbacks of the three. Activated carbon (AC) is materials that frequently utilized as a supercapacitor electrode due to the high surface area. Metal oxides such as manganese dioxide (MnO_2) with high teoritical specific capacitance which loaded in activated carbon will caused an improvement on supercapacitors electrochemical performance. The composite was fabricated using blending method with a mass difference of MnO_2, then deposited on a porous Ni-foam substrate. Ni-foam pores play as main role on the process of transferring electrolyte ions in the system so that the AC/MnO_2 has, resulting a supercapacitor based AC-MnO_2 15% nanocomposite with a gravimetric capacitance, energy density and power density of 79 F/g at 1 A/g, W/kg and Wh/kg respectively. The cell could maintain up to 93% after 100 cycles.

1 Introduction

The rising demand for energy in past few decades has led to major fossil fuel consumption and significant environmental pollution issues [1], [2]. The world's oil reserves are continuously being depleted as a result of overexploitation, which has become a well-known open secret in the energy sector. This is due to an increase in the number of machines and vehicles being produced that use oil as their primary energy source. In line with the demands of contemporary society and solve increasing ecological concerns, it is now crucial to develop cheap, innovative, and eco-friendly energy conversion and storage systems; this is why research in this area is progressing so quickly [3]. Supercapacitor has drawn a lot of attentiveness in a number of novel applications, including flexible and wearable technology, power backup systems, and electric vehicles [4], [5]. Their outstanding capabilities, such as extremely high power density, long cycle life, ultrafast recharging, and eco-friendly [6]–[9], have attracted much attention. They still have a low energy density, which significantly limits their commercialization. Therefore, it is extremely beneficial to investigate high energy density supercapacitors that will accommodate future energy demands and as well as bearing in mind that batteries have a higher energy density than supercapacitors, so the possibility of combining the two in the future should not be ruled out.

The most frequently used material in supercapacitors is activated carbon (AC), which has a large surface area (1000–3000 m^2g^{-1}) and a relatively high packing density (0.3–0.6 gcm^{-3}) [10]. Two significant drawbacks of AC materials, however slow charge transfer and the low electrical conductivity of ACs (10-100 Sm^{-1}) remain in the way of commercial AC-based supercapacitors ability to store energy [11]. So, in order to make up for the shortcomings of AC, other materials are required, such as transition metal oxides (TMOs). The relatively high theoretical specific capacity of TMO has raised interest through them as super capacitor electrode materials [12]. Numerous TMO, including ruthenium oxide (RuO_2) [13], nickel dioxide (NiO_2) [14], molybdenum disulfide (MsO_2), cobalt oxide (Co_3O_4) [15], manganese III oxide (Mn_2O_3) [16] and titanium dioxide (TiO_2) [17], have been widely used as the active materials owing to their high capacitance (above 1000 F/g) and superior charge transfer process. However, although RuO_2 has a theoretical specific capacitance of up to 2000 F/g, it has the drawbacks of high cost and toxicity. [18]. NiO's high resistivity is a huge handicap for super capacitors applications [19]. The main concern of Co_3O_4 is related to its poor cycle life and structural rigidity as a result of cycling-induced swelling and shrinkage [20]. TiO_2 have received positive interest as cutting-edge electrode materials in super capacitors, but they have low capacitance and poor conductivity [21]. Hence, MnO_2, a significant TMO, is an excellent material for super capacitor electrodes because it is inexpensive [22], environmentally friendly [23], and has a high specific capacitance (1380 Fg^{-1} of theoretical specific capacitance) [24].

*Corresponding author: markus.diantoro.fmipa@um.ac.id

In attempt to develop composites with superior properties, this research will vary the weight mass of MnO_2 incorporated to the AC material. The AC-MnO_2 composite was synthesized using simple mixing method and deposited onto nickle foam substrate.

2 Method

2.1 Nanocomposite AC-MnO_2 electrode paste preparation

Electrode paste synthesis was carried out using a simple mixing method, using commercially available materials. Activated carbon (AC), carbon black (CB), manganese dioxide (MnO_2), polyvinylidene fluoride (PVDF), dimethylacetamide (DMAc), acetonitrile (ACN), tetraethylammonium tetrafluoroborate (Et_4NBF_4), were used without any purification. The ratio Activated carbon and MnO_2, Carbon Black and polyvinilidene fluoride is 8:1:1. The weight mass of MnO_2 used varied by 10, 15, and 20%. The composite paste was made by dissolving PVDF and DMAc, which was then slowly filled with activated carbon and carbon black. At room temperature, the paste is then stirred for an additional seven hours. After Ni-foam substrate is sonicated for 1 hour with alcohol, it has to be dried. Afterward, the previously used paste was applied to Ni-foam with a constant amount throughout all variations. After that, the electrodes were heated for 1 hour in 100°C.

2.2 Devices fabrication

A two-electrode system is used to measure the performance of the electrodes by fabricate in coin cell. The electrodes were first applied with a specific amount of pressure before going to spend 24 hours immersed in a 1M Et_4NBF_4/ACN electrolyte solution. The coin cell is then assembled to generate a device that is ready to be tested afterwards.

2.3 Characterization

The characterization used during the analysis process includes X-ray diffractometer (PAN Analytical X'pert PRO) to get structural information such crystalinity, scanning electron microscopy (Inspect S50) to determine the shape of MnO_2, then cyclic voltammetry (PGSTAT302N) and galvano static charge discharge (Neware) to examine its electrochemical performance.

2.4 Calculation

The gravimetric capacitance (C, $F.g^{-1}$), gravimetric specific energy density (E, $Wh.kg^{-1}$) and power density (P, $Wh.kg^{-1}$) from the galvanostatic charge-discharge was calculated using equation below.:

$$C = \frac{4I\Delta t}{m\Delta V} \quad (1)$$

$$E = \frac{1}{8}\frac{C\Delta V^2}{3.6} \quad (2)$$

$$P = \frac{E\times 3600}{\Delta t} \quad (3)$$

where m is the mass of active material (g) on both electrodes, I is the discharge current (A), t is the discharge time (s), and V is the voltage (V), excluding the ohmic (IR) drop.

3 Results and discussion

3.1 Structural analysis

XRD can be used to determine material structure. Figure 1 shows the MnO_2 and activated carbon XRD diffraction pattern. MnO_2 and activated carbon's diffraction patterns both show amorphous structures, which are indicated by the lack of any sharp peaks remaining lot of irregular low peaks.

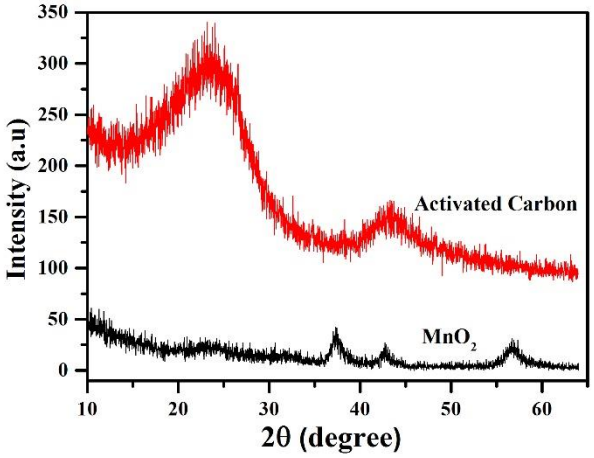

Fig 1. X-Ray dissfractionpattern of activated carbon and MnO_2

The X-ray diffraction pattern shows that MnO_2 has ramsdellite peaks (γ-MnO_2) at 2θ=37° matching with the (021) plan [25]. On the other hand, activated carbon has weak peaks at 2θ=26° and 44°. Based on the data above, its confirm that both activated carbon and γ-MnO_2has an amorphous structures [26].

Figure 2 shows the morphology of manganese dioxide as determined by SEM analysis. MnO_2 is spherical with a particle size of 4.2 nm

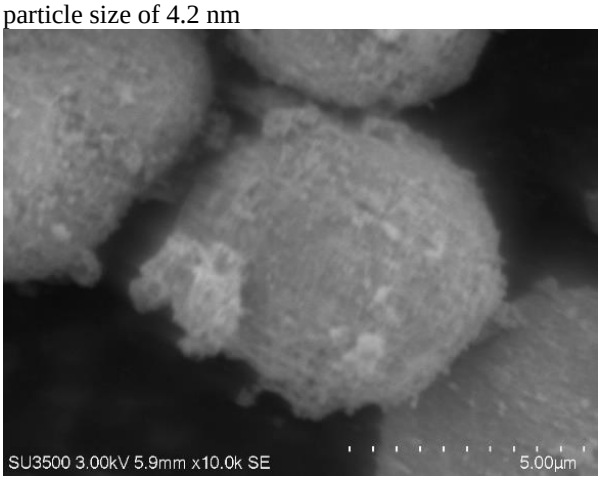

Fig 2. MnO_2 morphology through SEM analysis

3.2 Electrochemical performance

Two characterization methods, CV and GCD, can be used to determine the electrode's electrochemical performance. An organic electrolyte, 1M Et_4NBF_4, was utilized. The maximum voltage used for the test is 2 V. The results of the cyclic voltammetry test are shown in Figures 3 and 4 below for each cell.

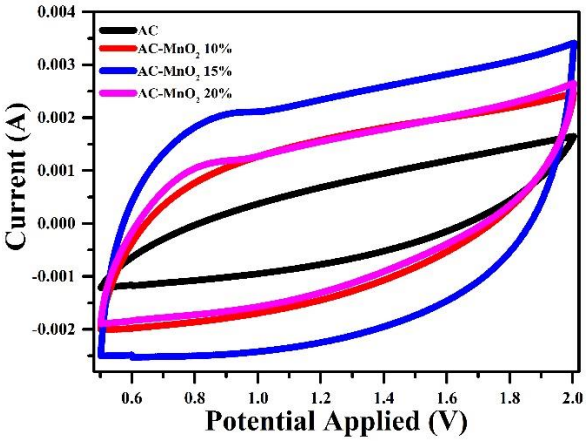

Fig 3. Cyclic curve of AC and AC-MnO_2 10-15% at low scan rate of 10 mV/s.

The cyclic curve confirm the composite's electrochemical behavior. Over all varieties in weight mass MnO_2, the CV curve has a semi-rectangular shape. This exemplifies the characteristics of the activated carbon-based EDLC material. However, there was a defect in the CV curve when the 15 and 20% AC-MnO_2 composite electrode reached a voltage of 0.9 V. This tends to result from the properties of the MnO_2-derived pseudo capacitive material. The characteristic behavior of EDLC-pseudo capacitance work in the cell is demonstrated on Figure 4 below. These deformations demonstrate that the electrolyte and MnO2 undergo a redox reaction. Despite the fact that activated carbon material makes up primary of the electrode, this characteristic may indicate that an addition of MnO_2 will affect electrode's electrochemical behavior.

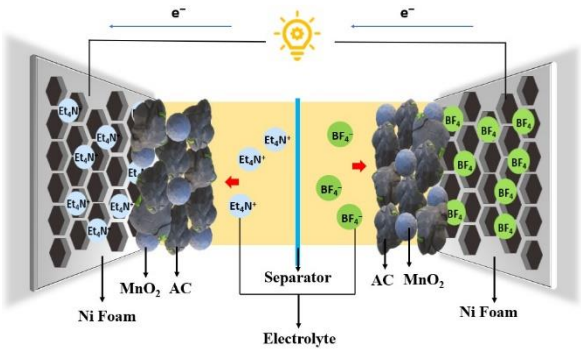

Fig 4. Illustration scheme of EDLC and pseudocapacitance behavior in AC-MnO_2 composite electrode with Ni-foam as the substrate

The area of the curve in relation to its shape has an impact on the electrode's performance as well. A wider CV curve enhances the electrochemical system's performance. The CV results in Figure 3 make it clearly apparent that the addition of the MnO_2 material significantly changes the area of the CV curve. The 15% AC-MnO_2 composite achieves the most optimal area, demonstrating that it is the best, compared to the others.

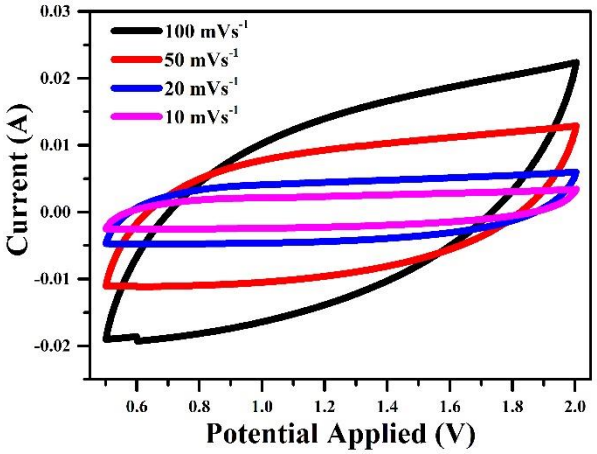

Fig 5. Cyclic voltammetry curve of AC-MnO_2 15% electrode in different scan rate.

The stability of the electrode's electrochemical process is assessed using the CV test in figure 5. However, as the scan rate increases, the shape of the entire curve changes. At low scan rates, the semi-quasi-rectangular shape is preserved. When the scan rate is increased, the curve becomes more pronounced at the edge because there isn't enough electrolyte ion diffusion [27]. The electrochemical reaction struggles at high scan rates because electrolyte ions are unable to pass through the pores [28].

The GCD curve provides the electrodes electrochemical properties. According to Figure 6, the discharge time increases as MnO_2 concentration rises to 15% for each weight mass variation. This demonstrates good electrochemical properties. However, the discharge time is reduced with the addition of 20% MnO_2, leading to the conclusion that 15% MnO_2 is the ideal MnO_2 composition.

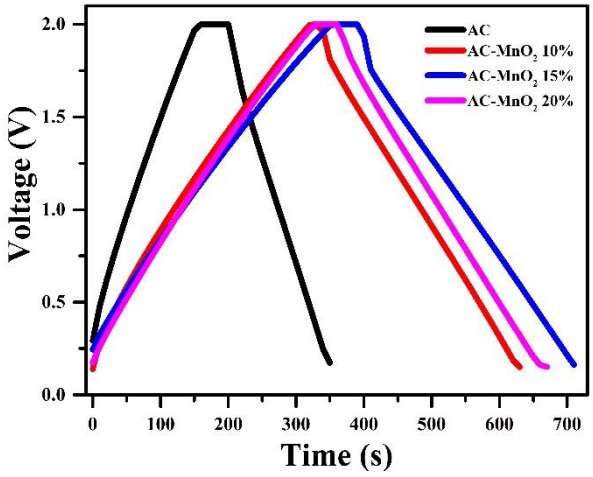

Fig 6. Charge discharge curve of AC-MnO_2 composite and activated carbon eletrodes in different weight mass (10-20%).

According to equations 1, 2, and 3, the electrochemical parameter of each composite were calculated and are displayed in table 1 below.

Table 1. Electrochemical parameter of AC and AC-MnO_2 10-20% composite based on charge-discharge curve calculation.

Sample	Gravimetric capacitance (F/g)	Energy density (Wh/kg)	Power density (W/kg)
AC	58.61	7.05	68.01
AC-MnO_2 10%	75.71	7.61	78.56
AC-MnO_2 15%	79.08	9.14	94.79
AC-MnO_2 20%	73.18	8.55	67.88

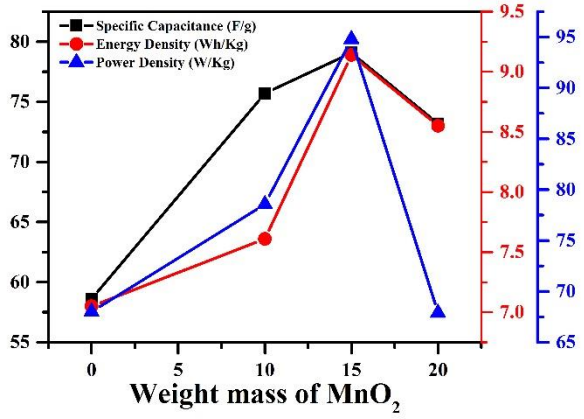

Fig. 7. Comparation of the electrochemical parameter of each MnO_2 weight mass

Figure 6 generates a graph from the electrochemical parameter data in table 1 to make it simpler to read the ideal electrode composite composition. The 15% AC-MnO_2 coin cell has superior gravimetric capacitance, 79.08 F/g. The 15% AC-MnO_2 composite had an energy density of 9.14 Wh/kg.

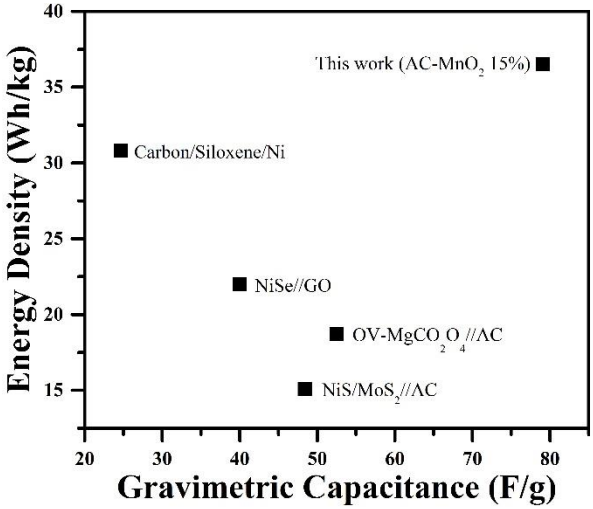

Fig 8. Comparison of the current investigation's gravimetric capacitance and energy density with a different research study [29]–[32]

Figure 7 explicitly states that 15% AC/MnO_2 performs significantly better than previous research. A hollow Ni-foam substrate also supports for this good performance as compared to the active material (figure 4).

This hollow structure strongly supports the electrode's electrochemical process. The use of Ni-foam as a substrate has many benefits due to its electrical conductivity and outstanding mechanical flexibility. Ni-foam exhibits outstanding stability as well as excellent corrosion and oxidation resistance. [33]. Ni-foam offers excellent mass transfer of the electrolyte with a relatively low contact resistance and improves the effective electron transport for supercapacitors [34]. These outcomes are consistent with earlier research that used aluminum foil substrates with varied th weight mass of MnO_2. On aluminum foil substrate, 15% AC-MnO_2 can be delivered power density of 85.44 W/kg [35]. This demonstrates that the performance of the device with Ni-foam substrate is better to aluminum foil even though their differences are relatively small.

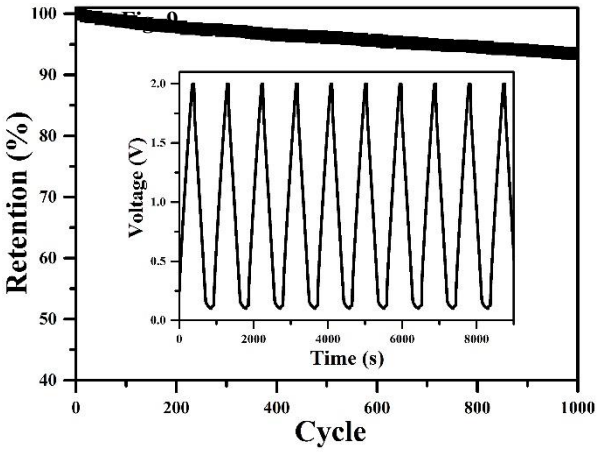

Fig. 9. Coulombic efficiency curve measured at 1 A/g for 100 cycles.

Figure 8 shows the coulombic efficiency of AC-MnO_2 15% device, measured at 1 A/g. The device could maintain up to 93% after 100 cycles, revealing an excellent electrochemical performance.

4 Conclusion

Supercapacitors with activated carbon active material, as well as composites with MnO_2 are able to produce good devices. The most optimum electrochemical performance of supercapacitor devices is achieved by 15% AC-MnO_2 composite with gravimetric capacitance of 79.08 F/g. This high performance is inseparable from the role of the Ni-foam substrate which facilitates electrolyte transport to be faster. The results of this study can help the researchers for future research to create even better energy storage systems. The outcomes of this study show that supercapacitors perform excellently. It may be possible to create better energy storage devices by combining supercapacitors with other energy storage technologies, such as batteries.

Acknowledgment

This work was supported by the research fund of the Internal UM grant program project No. 18.5.60/UN32/KP/2022. This work constitutes part of MDP research team.

References

1. L. Chen *et al.*, "A high-energy, long cycle life aqueous hybrid supercapacitor enabled by efficient battery electrode and widened potential window," *J. Alloys Compd.*, vol. 877, p. 160273, 2021.
2. I. Luthfiyah *et al.*, "The effect of spincoating speed on ZnONR microstructure and it's potential of ZnONR/Aluminum foil electrodes symmetric supercapacitors," *J. Phys. Conf. Ser.*, vol. 1595, no. 1, 2020.
3. A. Afif, S. M. Rahman, A. Tasfiah Azad, J. Zaini, M. A. Islam, and A. K. Azad, "Advanced materials and technologies for hybrid supercapacitors for energy storage – A review," *J. Energy Storage*, vol. 25, no. April, p. 100852, 2019.
4. Q. Zong *et al.*, "Three-dimensional coral-like NiCoP@C@Ni(OH)2 core-shell nanoarrays as battery-type electrodes to enhance cycle stability and energy density for hybrid supercapacitors," *Chem. Eng. J.*, vol. 361, pp. 1–11, Apr. 2019.
5. M. Chuai, X. Chen, K. Zhang, J. Zhang, and M. Zhang, "CuO-SnO 2 reverse cubic heterojunctions as high-performance supercapacitor electrodes," *J. Mater. Chem. A*, vol. 7, no. 3, pp. 1160–1167, 2019.
6. S. Ghosh, S. M. Jeong, and S. R. Polaki, "A review on metal nitrides/oxynitrides as an emerging supercapacitor electrode beyond oxide," *Korean J. Chem. Eng.*, vol. 35, no. 7, pp. 1389–1408, 2018.
7. N. R. Chodankar *et al.*, "Potentiodynamic polarization assisted phosphorus-containing amorphous trimetal hydroxide nanofibers for highly efficient hybrid supercapacitors," *J. Mater. Chem. A*, vol. 8, no. 11, pp. 5721–5733, 2020.
8. S. E. I. Suryani, N. Sholeha, T. Suprayogi, A. Taufiq, N. Mufti, and M. Diantoro, "Magnetocapacitance of FC-ATiO3(A = Ba, Ca, Sr) for supercapacitor electrode," *AIP Conf. Proc.*, vol. 2251, no. August, 2020.
9. F. U. Zuhri *et al.*, "ZnO-FC-NiCo MOF for prospective supercapacitor materials," *Mater. Today Proc.*, vol. 44, pp. 3385–3389, 2020.
10. P. Wang *et al.*, "Porous carbon for high-energy density symmetrical supercapacitor and lithium-ion hybrid electrochemical capacitors," *Chem. Eng. J.*, vol. 375, 2019.
11. C. Li *et al.*, "Scalable combustion synthesis of graphene-welded activated carbon for high-performance supercapacitors," *Chem. Eng. J.*, vol. 414, p. 128781, Jun. 2021.
12. Q. Zong, C. Liu, H. Yang, Q. Zhang, and G. Cao, "Tailoring nanostructured transition metal phosphides for high-performance hybrid supercapacitors," *Nano Today*, vol. 38, p. 101201, 2021.
13. N. Wu *et al.*, "Recent Advances of Asymmetric Supercapacitors," *Adv. Mater. Interfaces*, vol. 8, no. 1, pp. 1–17, 2021.
14. H. Peçenek, F. K. Dokan, M. S. Onses, E. Yılmaz, and E. Sahmetlioglu, "Outstanding supercapacitor performance with intertwined flower-like NiO/MnO2/CNT electrodes," *Mater. Res. Bull.*, vol. 149, no. December 2021, p. 111745, 2022.
15. R. Kumar, S. Sahoo, W. K. Tan, G. Kawamura, A. Matsuda, and K. K. Kar, "Microwave-assisted thin reduced graphene oxide-cobalt oxide nanoparticles as hybrids for electrode materials in supercapacitor," *J. Energy Storage*, vol. 40, no. April, p. 102724, 2021.
16. L. Suryanti *et al.*, "The effect of Mn2O3nanoparticles on its specific capacitance of symmetric supercapacitors FC-ZnO-x(Mn2O3)," *Mater. Today Proc.*, vol. 44, pp. 3355–3360, 2020.
17. M. Diantoro, I. Luthfiyah, Istiqomah, H. Wisodo, J. Utomo, and W. Meevasana, "Electrochemical Performance of Symmetric Supercapacitor Based on Activated Carbon Biomass TiO2Nanocomposites," *J. Phys. Conf. Ser.*, vol. 2243, no. 1, 2022.
18. C. Zhang *et al.*, "A Facile Synthesis of TiO2-NiCo2S4-Ti3C2 Electrode material by Hydrothermal Method and its electrochemical performance for Supercapacitor Application," *Int. J. Electrochem. Sci.*, vol. 17, pp. 1–10, 2022.
19. T. Rakesh Kumar, C. H. Shilpa Chakra, S. Madhuri, E. Sai Ram, and K. Ravi, "Microwave-irradiated novel mesoporous nickel oxide carbon nanocomposite electrodes for supercapacitor application," *J. Mater. Sci. Mater. Electron.*, vol. 32, no. 15, pp. 20374–20383, 2021.
20. S. Zallouz, B. Réty, L. Vidal, J. M. Le Meins, and C. Matei Ghimbeu, "Co3O4Nanoparticles Embedded in Mesoporous Carbon for Supercapacitor Applications," *ACS Appl. Nano Mater.*, vol. 4, no. 5, pp. 5022–5037, 2021.
21. H. Shi *et al.*, "Free-standing integrated cathode derived from 3D graphene/carbon nanotube aerogels serving as binder-free sulfur host and interlayer for ultrahigh volumetric-energy-density lithium[sbnd]sulfur batteries," *Nano Energy*, vol. 60, pp. 743–751, 2019.
22. J. Miao *et al.*, "Electrochemical Performance of an Asymmetric Coin Cell Supercapacitor Based on Marshmallow-like MnO2/Carbon Cloth in Neutral and Alkaline Electrolytes," *Energy and Fuels*, vol. 35, no. 3, pp. 2766–2774, 2021.
23. A. K. Worku, D. W. Ayele, N. G. Habtu, M. A. Teshager, and Z. G. Workineh, "Recent progress in MnO2-based oxygen electrocatalysts for rechargeable zinc-air batteries," *Mater. Today Sustain.*, vol. 13, p. 100072, 2021.
24. H. Duan *et al.*, "When Conductive MOFs Meet MnO 2 : High Electrochemical Energy Storage Performance in an Aqueous Asymmetric Supercapacitor," 2021.
25. F. Moulai, O. Fellahi, B. Messaoudi, T. Hadjersi, and L. Zerroual, "Electrodeposition of nanostructured γ-MnO2 film for photodegradation of Rhodamine B," *Ionics (Kiel).*, vol. 24, no. 7, pp. 2099–2109, 2018.
26. X. Song, H. Duan, Y. Zhang, H. Wang, and H. Cao, "Facile synthesis of γ -MnO2/rice husk-based-activated carbon and its electrochemical properties," *Funct. Mater. Lett.*, vol. 10, no. 5, pp. 9–11, 2017.
27. P. H. Wadekar, R. V. Khose, D. A. Pethsangave, and S. Some, "One-pot Facile Synthesis of Sulfur and Nitrogen co- functionalized Graphene material using Novel Deep Eutectic Solvent for Supercapacitor applications some 2019.pdf," *Chem. Sustain. Chem.*, vol. 12, pp. 1–11, 2019.
28. Jjung jie Huang, Y. X. Zhang, and jun xiang Zhang, "Characterization of MnO2 and AgNWs Co-Doped into an Activated Carbon Thin Film Electrode for Supercapacitors," *J. Electron. Mater.*, vol. 50, no. 11, pp. 6535–6544, 2021.

29. K. Krishnamoorthy, M. S. P. Sudhakaran, P. Pazhamalai, V. K. Mariappan, Y. S. Mok, and S. J. Kim, "A highly efficient 2D siloxene coated Ni foam catalyst for methane dry reforming and an effective approach to recycle the spent catalyst for energy storage applications," *J. Mater. Chem. A*, vol. 7, no. 32, pp. 18950–18958, 2019.
30. J. Yan *et al.*, "Smart in situ construction of NiS/MoS2 composite nanosheets with ultrahigh specific capacity for high-performance asymmetric supercapacitor," *J. Alloys Compd.*, vol. 811, p. 151915, 2019.
31. [31]S. M. Dinara *et al.*, "Synthesis of a 3D free standing crystalline NiSeX matrix for electrochemical energy storage applications," *Dalt. Trans.*, vol. 48, no. 45, pp. 16873–16881, 2019.
32. H. Wang, N. Mi, S. Sun, W. Zhang, and S. Yao, "Oxygen vacancies enhancing capacitance of MgCo2O4 for high performance asymmetric supercapacitors," *J. Alloys Compd.*, vol. 869, p. 159294, 2021.
33. M. Diantoro, L. Suryanti, F. U. Zuhri, S. E. I. Suryani, and L. Chuenchom, "Manganese Oxide and Temperature Induced on Microstructure and Electrical Properties of Graphene-(Mn2O3)x-ZnO/Ni Foam," *IOP Conf. Ser. Mater. Sci. Eng.*, vol. 515, no. 1, 2019.
34. N. You *et al.*, "Constructing P-CoMoO4@NiCoP heterostructure nanoarrays on Ni foam as efficient bifunctional electrocatalysts for overall water splitting," *Nano Mater. Sci.*, no. April, pp. 1–9, 2021.
35. M. Diantoro *et al.*, "Hierarchical Activated Carbon – MnO 2 Composite for Wide Potential Window Asymmetric Supercapacitor Devices in Organic Electrolyte," 2022.